



Minerva Access is the Institutional Repository of The University of Melbourne

Author/s:

Mariani, M;Connor, SE;Fletcher, M-S;Theuerkauf, M;Kunes, P;Jacobsen, G;Saunders, KM;Zawadzki, A

Title:

How old is the Tasmanian cultural landscape? A test of landscape openness using quantitative land-cover reconstructions

Date:

2017-10-01

Citation:

Mariani, M., Connor, S. E., Fletcher, M. -S., Theuerkauf, M., Kunes, P., Jacobsen, G., Saunders, K. M. & Zawadzki, A. (2017). How old is the Tasmanian cultural landscape? A test of landscape openness using quantitative land-cover reconstructions. *Journal of Biogeography*, 44 (10), pp.2410-2420. <https://doi.org/10.1111/jbi.13040>.

Persistent Link:

<https://hdl.handle.net/11343/293046>

1
2
3
4
5
6
7
8
9
10
11
12
13
14
15
16
17
18
19
20
21
22
23

MISS MICHELA MARIANI (Orcid ID : 0000-0003-1996-3694)

Article type : Original Article

Journal of Biogeography

Article type: Original Article

Running head: Testing Holocene landscape openness in Tasmania

TITLE: How old is the Tasmanian cultural landscape? A test of landscape openness using quantitative land cover reconstructions.

Authors: Mariani M.¹, Connor, S.E.^{1,2}, Fletcher, M.-S.¹, Theuerkauf, M.³, Kuneš P.⁴, Jacobsen G.⁵,
Saunders, K.M.⁵, Zawadzki, A.⁵

¹School of Geography, University of Melbourne, Melbourne, Victoria, Australia

²Centro de Investigação Marinha e Ambiental (CIMA), University of the Algarve, Faro 8005-139, Portugal

³Institute for Geography and Geology, Ernst-Moritz-Arndt-University Greifswald, Greifswald, Germany

⁴Department of Botany, Faculty of Science, Charles University, 128 43 Prague, Czech Republic

⁵Australian Nuclear Science and Technology Organisation, Lucas Heights, New South Wales, Australia

This is the author manuscript accepted for publication and has undergone full peer review but has not been through the copyediting, typesetting, pagination and proofreading process, which may lead to differences between this version and the [Version of Record](#). Please cite this article as [doi: 10.1111/jbi.13040](https://doi.org/10.1111/jbi.13040)

This article is protected by copyright. All rights reserved

24 Correspondence to: MICHELA MARIANI, School of Geography, University of Melbourne, Victoria,
25 Australia; mmariani@student.unimelb.edu.au

26

27 WORD COUNT:7107

28

29 **Abstract**

30 **Aim** To test competing hypotheses about the timing and extent of Holocene landscape opening
31 using pollen-based quantitative land-cover estimates.

32 **Location** Dove Lake, Tasmanian Wilderness World Heritage Area, Australia.

33

34 **Methods** Fossil pollen data were incorporated into pollen dispersal models and corrected for
35 differences in pollen productivity among key plant taxa. Mechanistic models (REVEALS - Regional
36 Estimates of VEgetation Abundance from Large Sites) employing different models for pollen
37 dispersal (Gaussian plume and Lagrangian stochastic models) were evaluated and applied in the
38 Southern Hemisphere for the first time.

39

40 **Results** Validation of the REVEALS model with vegetation cover data suggests an overall better
41 performance of the Lagrangian stochastic model. Regional land-cover estimates for forest and non-
42 forest plant taxa show persistent landscape openness throughout the Holocene (average landscape
43 openness ~50%). *Gymnoschoenus sphaerocephalus*, an indicator of moorland vegetation, shows
44 higher values during the early Holocene (11.7-9 ka) and declines slightly through the mid-Holocene
45 (9-4.5 ka) during a phase of partial landscape afforestation. Rain forest cover reduced (from ~40% to
46 ~20%) during the period between 4.2 – 3.5 ka.

47 **Main conclusions** Pollen percentages severely under-represent landscape openness in western
48 Tasmania and this bias has fostered an over-estimation of Holocene forest cover from pollen data.
49 Treeless vegetation dominated Holocene landscapes of the Dove Lake area, allowing us to reject
50 models of landscape evolution that invoke late-Holocene replacement of a rain forest-dominated
51 landscape by moorland. Instead, we confirm a model of Late Pleistocene inheritance of open
52 vegetation. Rapid forest decline occurred after ca. 4 ka, likely in response to regional moisture
53 decline.

54 **Keywords**

55 Australia, cultural landscape, dispersal models, fire, Holocene, moorland, rain forest, REVEALS,
56 Tasmania, vegetation reconstruction

57 1. Introduction

58

59 The ability to accurately model and predict Earth system behaviour is crucial for developing effective
60 management strategies for our future environment (e.g. Anderson *et al.*, 2006; Dearing *et al.*, 2010;
61 Gaillard *et al.*, 2010). Recognition of the reciprocal relationship between vegetation cover and
62 climate via biogeochemical and biogeophysical processes/feedbacks (e.g. Foley *et al.*, 2003) has
63 fostered development of coupled dynamic vegetation and climate models (e.g. Smith *et al.*, 2011). A
64 critical point is the scarce information on past land cover currently incorporated into such models
65 (e.g. Kaplan *et al.*, 2002; Sitch *et al.*, 2003; Smith *et al.*, 2011). Quantitative estimates of past plant
66 cover are rare (e.g. Trondman *et al.*, 2015), with the Southern Hemisphere particularly under-
67 represented. Here we apply, for the first time in the Southern Hemisphere, mechanistic models for
68 regional vegetation reconstruction to quantify landscape changes in western Tasmania, Australia.
69 These reconstructions allow us to address biogeographical and methodological debates over a) the
70 efficiency of mechanistic models in landscapes dominated by both wind- and animal- pollinated
71 plants; and b) the timing and extent of long-term vegetation changes in western Tasmania.

72

73 Fire is considered the most critical non-climatic factor controlling land cover changes on Earth (Bond
74 *et al.*, 2005). Fire and vegetation are strongly linked in Australia (Bradstock *et al.*, 2002), with, for
75 example, the distribution of fire-sensitive rain forest among flammable sclerophyll vegetation
76 considered to be a result of the past fire history (Bowman, 1998; Bowman, 2000). Tasmania (Fig. 1) is
77 an exemplar of the role of fire in decoupling vegetation from climate, with large areas in which rain
78 forest is the potential vegetation currently occupied by fire-promoted vegetation (Jackson, 1968;
79 Brown & Podger, 1982a; Wood & Bowman, 2011). Indeed, the juxtaposition of fire-sensitive rain
80 forest against pyrogenic species (e.g. *Eucalyptus*) in Tasmania has puzzled ecologists for decades
81 (Bowman & Jackson, 1981; Brown & Podger, 1982b; Yospin *et al.*, 2015) and the origin and evolution
82 of the present-day dominance of pyrogenic moorland is the subject of long-standing debate (see
83 Colhoun, 1996a; Fletcher & Thomas, 2010a; Macphail, 2010 and references therein). This debate is
84 split between those that argue for late Holocene replacement of a forested landscape by open
85 vegetation (Macphail, 1979; Colhoun, 1996b), while others argue an open landscape persisted
86 throughout the Holocene (Thomas, 1995a; Fletcher & Thomas, 2010a).

87 Proponents of the former model interpret the region-wide dominance of rain forest pollen types as
88 indicating a climate-driven expansion of rain forest from the Late Pleistocene to the mid-Holocene
89 (e.g. Macphail, 1979; Colhoun, 1996). In contrast, Fletcher & Thomas (2007a, b; 2010a, b) highlight
90 the bias in the pollen record toward plants that produce large amounts of well-dispersed pollen (i.e.
91 rain forest species in Tasmania), and use modern pollen spectra to infer the persistence of open
92 vegetation across western Tasmania for the last ca. 12,000 years (12 kyrs). They note a departure
93 between Holocene and previous interglacial floras and charcoal sequences, citing human arrival
94 during the last glacial cycle (~35 kyrs) as the probable cause for this, thus concluding that western
95 Tasmania represents an ancient cultural landscape. Macphail (2010) has critiqued their model,
96 arguing that the nature of pollen deposition at many of the mires studied by Fletcher and Thomas
97 (2010) biases pollen records toward local bog vegetation, which is palynologically similar to
98 pyrogenic moorland. Thus, the debate over the origin and development of the modern treeless and
99 pyrogenic vegetation landscape of western Tasmania centres on how pollen production and
100 deposition biases are resolved.

101

102 Here, we produce quantitative land cover estimates to understand vegetation change and test
103 competing models of landscape evolution in western Tasmania. We employ recently reported
104 pollen productivity estimates (PPEs) for this region (Mariani *et al.*, 2016) to develop quantitative land
105 cover estimates using the REVEALS (Sugita, 2007b) approach.

106

107 **1.1 Quantitative reconstruction of land cover from pollen data**

108 Quantitative reconstruction of past vegetation cover has long been a major objective of palynology
109 (e.g. Sugita, 1993; Gaillard *et al.*, 1998; Broström *et al.*, 2004). Numerous factors influence the over-
110 or under-representation of vegetation in pollen spectra (e.g. taphonomy, pollen productivity,
111 dispersal capabilities) (Fletcher & Thomas, 2007b; de Nascimento *et al.*, 2015). Recent advances
112 enable effective modelling of pollen productivity and dispersal (Sugita, 2007a, b; Gaillard *et al.*,
113 2010), improving understanding of past vegetation dynamics and providing quantitative land-cover
114 data to landscape management and palaeoclimate modelling. Emerging from these efforts is the
115 landscape reconstruction algorithm (LRA: Sugita 2007a,b) for estimating vegetation abundance on
116 regional (10^4 - 10^5 km² –REVEALS model) and local (<1 km² up to 5 km² –LOVE model) scales. These
117 mechanistic models employ pollen productivity estimates (PPEs) to correct productivity bias, and
118 models of dispersal and deposition of small particles in the air, to correct differences in pollen
119 dispersion.

120

121 The main assumption behind REVEALS, supported by simulations and empirical studies, is that pollen
122 deposited in large sites (>50-100 ha) originate from a larger source-area (Jacobson & Bradshaw,
123 1981), and can be used to estimate regional vegetation cover (Sugita, 2007b; Hellman *et al.*, 2008). A
124 critical choice is the pollen dispersal model. The most commonly employed dispersal model in the
125 REVEALS approach is the Gaussian plume model (REVEALS-GPM) (Prentice, 1985; Sugita, 1993;
126 Sugita, 1994; Sugita, 2007a), while the emerging Lagrangian stochastic model (REVEALS-LSM) has
127 only been employed in Germany thus far (Kuparinen *et al.*, 2007; Theuerkauf *et al.*, 2013). The GPM
128 uses Sutton's air pollutant plume dispersion equation (Sutton, 1953) and describes the concentration
129 of particles downwind from a point source as spreading outward from the centreline of the plume
130 following a normal distribution. This model may be less reliable for particle dispersal over longer
131 distances, due to the influence of vertical airflows and turbulence (Kuparinen *et al.*, 2007). The LSM
132 is fully mechanistic dispersal model that more realistically describes pollen dispersal and deposition
133 in lakes (Theuerkauf *et al.*, 2013). Both models were previously employed in Tasmania to derive
134 pollen productivity estimates; LSM was found to perform more realistically (Mariani *et al.*, 2016).

135

136 Quantifying landscape openness from palynological data is a long-awaited goal (Faegri & Iversen,
137 1989). In Europe, the ratio between Arboreal Pollen (AP) and Non-Arboreal Pollen (NAP) has
138 traditionally been used to qualitatively describe human impact on landscapes. However, pollen
139 percentages and AP:NAP relationships are not linearly related to vegetation composition and
140 landscape patterns (e.g. Sugita *et al.*, 1999; Hellman *et al.*, 2008) and the proportion of unforested
141 land is strongly underestimated by NAP data (Hellman *et al.*, 2008; Kuneš *et al.*, 2011; Kuneš *et al.*,
142 2015). An attempt to correct for this bias in southern Sweden revised NAP-based estimates of 30-
143 40% open vegetation to 60-80% using REVEALS (Hellman *et al.*, 2008; Gaillard *et al.*, 2010).

144

145 REVEALS development and validation have mainly occurred in the Northern Hemisphere (e.g.
146 Hellman *et al.*, 2008; Sugita *et al.*, 2010; Abraham & Kozáková, 2012; Mazier *et al.*, 2012; Hultberg *et al.*
147 *et al.*, 2015; Trondman *et al.*, 2015), where most plant species are wind-pollinated and the goal has
148 been quantifying human impact on vegetation. To date, no attempt has been made to quantitatively
149 reconstruct land cover changes in the Southern Hemisphere using pollen dispersal models, nor in
150 vegetation with numerous animal-pollinated plants (e.g. *Eucalyptus*), such as in Tasmania. In this
151 paper, we apply and validate REVEALS-LSM and REVEALS-GPM to reconstruct Holocene
152 vegetation/land cover in the Southern Hemisphere for the first time.

153

154 **2. Methods**

155

156 2.1 Study area

157 Tasmania is a cool temperate island located around 300 km south of mainland Australia. The island is
158 bisected by a north-west/south-east trending mountain range, which produces a steep orographic
159 precipitation gradient with a wet west and dry east (Gentilli, 1972; Sturman & Tapper, 2006). Mean
160 annual temperature in the west varies from 5-7°C (winter) to 14-16°C (summer) and precipitation
161 values exceed 3000 mm (Australian Bureau of Meteorology, <http://www.bom.gov.au/>). Presently,
162 western Tasmania is dominated by treeless pyrogenic vegetation (moorland), whereas rain forest
163 communities are restricted by topography and fire protection (Wood *et al.*, 2011a). The main
164 component of current moorland vegetation in western Tasmania is buttongrass (*Gymnoschoenus*
165 *sphaerocephalus* Brown/Hooker (Cyperaceae)).

166

167 Dove Lake (41°39'34.27"S, 145°57'35.14"E; *Wee bone ne tinker* in the local indigenous language) lies
168 beneath the iconic Cradle Mountain (*War loun dig er ler*) within the World Heritage-listed Cradle
169 Mountain-Lake St. Clair National Park. Humans settled here >35 kyrs ago (Cosgrove, 1999) and
170 Cradle Mountain was the last place in Tasmania's west occupied by Tasmanian Aborigines prior to
171 their exile in the 19th century (Plomley, 1966). Dove Lake is medium-sized (90 ha), subalpine lake
172 (940 m a.s.l.) of glacial origin (Fig. 1, S1) and surrounded by steep topography (Fig. S1). Dove is one
173 of the largest natural lakes in western Tasmania; its size makes it suitable for regional vegetation
174 reconstruction using REVEALS (e.g. Sugita, 2007b; Hellman *et al.*, 2008). Mean annual rainfall at the
175 nearest meteorological station (Cradle Valley; 41°38'24.23"S, 145°56'24.28"E; 903 m a.s.l.) is 2698
176 mm (Fig. 1).

177

178 The vegetation around Dove Lake is dominated by sclerophyllous heath and *Eucalyptus* woodlands
179 on the eastern and western flanks; moorland is found at the northern edge and rain forest only
180 occupies the south-west corner (Fig. 1b). Dominant species in the modern landscape are *Eucalyptus*
181 *coccifera* Hook., *Lophozonia cunninghamii* Hook. (syn. *Nothofagus cunninghamii*), *Gymnoschenous*
182 *sphaerocephalus* and various ericaceous shrubs. Typical montane rain forest trees are also found,
183 such as *Fuscospora gunnii* Hook. (syn. *Nothofagus gunnii*), *Athrotaxis selaginoides* D.Don and *A.*
184 *cupressoides* D.Don (Cupressaceae). In this paper the genus name *Nothofagus* will be used when
185 referring to *Lophozonia* and *Fuscospora* in order to maintain consistency with fossil records (Hill *et*
186 *al.*, 2015).

187

188

189 **2.2 Pollen and charcoal analysis**

190

191 Pollen, spore and microscopic charcoal sample preparation followed standard protocols (Faegri &
192 Iversen, 1989) at 1-cm intervals. Relative pollen data were calculated from a pollen sum of at least
193 300 terrestrial pollen grains per sample (excluding wetland taxa and ferns). Microscopic charcoal
194 was counted on the microscope slides during pollen counting. Macroscopic charcoal was analysed at
195 5 mm-resolution to reconstruct local fire history. A set amount of sediment (1.25 cm³) per sample
196 was digested in 5% Sodium Hypochlorite (bleach) for at least two weeks and sieved using 125- μ m and
197 250- μ m diameter meshes (Whitlock & Larsen, 2001). To account for variations in sediment
198 deposition, charcoal counts were converted into Charcoal Accumulation Rates (CHAR, particles cm⁻²
199 yr⁻¹).

200

201 **2.3 Quantitative vegetation reconstruction and model validation**

202

203 The choice of dispersal model in REVEALS is crucial (Theuerkauf *et al.*, 2013). The Gaussian plume
204 model (Prentice, 1985; Sugita, 1993; Sugita, 1994) and the Lagrangian stochastic model (Kuparinen
205 *et al.*, 2007) are the two models currently implemented in PPE calculations and REVEALS runs
206 (REVEALS-GPM and REVEALS-LSM). Compared to the GPM, the LSM gives greater importance to
207 pollen arriving from longer distances (Kuparinen *et al.*, 2007; Theuerkauf *et al.*, 2013). Pollen fall
208 speed (terminal velocity) also has a large effect on predicted dispersal in the GPM, yet a small effect
209 in the LSM (Theuerkauf *et al.*, 2013).

210

211 We validated the models' vegetation estimates from two surface sediment samples from large lakes
212 (Dove Lake and Lake St Clair – Hopf *et al.*, 2001) against the actual vegetation cover around the same
213 lakes and pollen data (see Hellman *et al.* 2008) using principal component analysis (PCA; Jolliffe,
214 2002). Lake St Clair (Fig.1) is the largest natural lake (4500 ha) in western Tasmania and expected to
215 register regional vegetation information. REVEALS modelling employed recently published PPEs and
216 fall speeds for thirteen key pollen taxa in western Tasmania (Mariani *et al.* 2016). In addition to the
217 regional average wind speed of 6.5 m/s, we calculated additional GPM-based PPEs for a wind speed
218 of 3 m/s to compare with published estimates. For the LSM, we calculated PPEs with parameters for
219 windy conditions (see Kuparinen *et al.*, 2007) to compare with the published LSM-based PPEs

220 calculated with parameters for unstable conditions (see Mariani *et al.*, 2016). Thus we assess four
221 modelled atmospheric scenarios: GPM 3 m/s, GPM 6.5 m/s, LSM unstable and LSM windy unstable.

222
223 All model runs were performed in the 'discover' package (Theuerkauf *et al.*, 2016) for R v.3.3.1 (The
224 R foundation for Statistical Computing, 2016). Plant cover percentages around the target lakes were
225 calculated for a 50 km-radius (approximately the area covered by the REVEALS reconstruction) using
226 the vegetation map, TasVeg 3.0 (Government of Tasmania, 2013) in ARCMAP 10.2 (ESRI -
227 Environmental Systems Resource Institute, 2009, Redlands, California) and plant survey data
228 (Mariani *et al.* 2016). Validation employed principal component analysis (PCA) in PC-ORD FOR
229 WINDOWS 4.27 (McCune & Mefford, 1999). Detrended Correspondence Analysis (DCA) was
230 performed in the R package 'vegan' (Oksanen *et al.*, 2015) to confirm that PCA was appropriate
231 (Birks *et al.*, 2012). Pollen percentages from the two surface samples were also added to the analysis
232 to gauge model improvement. Mean deviation from actual plant cover (%) was also calculated for
233 each taxon.

234
235 For REVEALS application to the Dove Lake fossil record, all taxa from Mariani *et al.* (2016) were used
236 (excluding infrequent <1% taxa: *Monotoca*, *Sprengelia* and *Eucryphia*), accounting for at least 80% of
237 the terrestrial pollen counts per sample. To assess the performance of REVEALS under different
238 atmospheric scenarios, REVEALS was applied to the Holocene pollen data from Dove Lake using the
239 four model settings mentioned above. Plant taxa were grouped into forest and non-forest
240 categories based on structure (Table 1).

241

242 3. Results

243

244 3.1 Pollen and charcoal analysis

245 Pollen, spores and microscopic charcoal were analysed in 109 samples. A reduced pollen diagram
246 showing only key taxa for vegetation reconstruction appears in Fig. 2. For comparison with REVEALS
247 results, key taxa were re-scaled to 100%. The full, non-rescaled pollen diagram with pollen zone
248 descriptions appears in Fig. S3 and S4.

249 Pollen abundances of montane rain forest indicators (*Cupressaceae* and *Nothofagus gunnii*) show a
250 persistent decline from early to late Holocene. Pollen of the main rain forest component today,
251 *Nothofagus cunninghamii*, shows high values (~50%), until ca. 4 ka, and then declines to 25%. Pollen

252 of *Phyllocladus aspleniifolius* Hooker increases from the early to mid-Holocene, with an evident
253 decline since ca. 5 ka. *Eucalyptus* pollen is relatively abundant throughout the sequence, with a
254 stepwise increase at around ca. 5 ka. Pollen percentages of non-forest taxa are consistently low
255 (<20%): Poaceae and *Bauera rubioides* increase after ca. 5 ka, together with pollen of
256 *Gymnoschoenus sphaerocephalus*. *G. sphaerocephalus* pollen is most abundant during the early
257 Holocene (~8%), somewhat rarer throughout the mid-Holocene, and again more abundant after ca.
258 5 ka. Total forest pollen increases from early to mid-Holocene, reaching 85% of the total terrestrial
259 pollen spectrum. During the late Holocene, rain forest pollen declines substantially to 40-60%.

260 Macroscopic CHAR values are generally low throughout the core, with substantial peaks at 3.7, 4.5
261 ka and relatively high macroscopic charcoal influx between 6.5 and 7.5 ka (Fig. 2). Micro-CHAR peaks
262 are mainly synchronous with macro-CHAR peaks, both showing a sharp increase during the last 160
263 years preceded by periods of high microscopic charcoal influx between 3.4-4 ka, 5.8-6.3 ka and
264 peaks at 7.2 ka and 10.8 ka (Fig. 2).

265

266 **3.3 REVEALS validation**

267 PPEs calculations under atmospheric settings different from the published material (Table 1) appear
268 in Table S3. Differences between REVEALS estimates and predicted vegetation cover (%) are
269 presented in Fig. S4 and S5. PPEs calculated with GPM 3 m/s and GPM 6.5 m/s show large
270 differences, whereas PPEs from LSM under unstable and windy conditions are quite similar.
271 Vegetation cover errors (%) are generally smaller for the REVEALS-LSM runs, compared to REVEALS-
272 GPM (Fig. S4 and S5).

273

274 REVEALS validation appears in Fig. 3. PCA axis 1 clearly isolates pollen percentages, modern plant
275 cover and REVEALS results for GPMs and LSMs. *Gymnoschoenus sphaerocephalus* and *Eucalyptus*
276 show the strongest correlations with Axis 1, $r=0.98$ and $r=-0.89$ respectively, whereas Ericaceae and
277 *Nothofagus cunninghamii* are correlated with Axis 2, $r=0.85$ and $r=-0.71$ respectively. The majority of
278 pollen taxa align along Axis 2, clearly separating anemophilous (skewed towards *N. cunninghamii*)
279 and zoophilous taxa (skewed towards Ericaceae). Zoophilous taxa are positioned close to results for
280 REVEALS-LSM and REVEALS-GPM 6.5 m/s and modern plant cover, whereas wind-pollinated taxa are
281 skewed towards pollen percentages. REVEALS-LSM (both unstable and windy conditions) and
282 REVEALS-GPM (6.5 m/s) estimates for Lake St. Clair are close to the actual plant cover extracted
283 from a 50-km buffer from this site. The PCA biplot shows REVEALS GPM performs better using 6.5
284 m/s wind speed than 3 m/s. Current plant cover around Dove Lake and Lake St Clair is more closely

285 related with REVEALS-LSM results than REVEALS-GPM results on Axis 1, suggesting an overall better
286 performance of LSM. Interestingly, the two runs for REVEALS-LSM are virtually identical, whereas the
287 REVEALS-GPM runs are separated on the PCA biplot.

288

289 **3.4 REVEALS application**

290

291 Figure 4 summarises pollen percentages and REVEALS estimates obtained using GPM and LSM for
292 forest and non-forest taxa. REVEALS estimates for single taxa are presented in Fig. S6 and S7,
293 alongside effects of different atmospheric parameters (Fig. S8). REVEALS-LSM provides more
294 coherent cover estimates than REVEALS-GPM (Fig. S8). Given the validation results, we focus on the
295 results of REVEALS-GPM (6.5 m/s) and REVEALS-LSM (unstable) to address long-term landscape
296 dynamics at Dove Lake.

297

298 GPM estimates show high land-cover for *G. sphaerocephalus* (solid red, Fig. 4), a moorland indicator,
299 reaching more than 60%. Rain forest cover (light green, Fig. 4) is relatively low, accounting for less
300 than 40% throughout the Holocene. *Eucalyptus* (dark green, Fig. 4), an indicator of sclerophyll
301 forests, covers less than 5% throughout the reconstruction period. LSM dispersal simulations
302 produce markedly different results: *G. sphaerocephalus* covers up to 45% of total reconstructed land
303 cover, forest cover varies between ~20% and ~40% and *Eucalyptus* cover is fairly constant between 5
304 and 10% throughout the reconstruction period. Both model runs show maximum forest cover
305 between 10 ka and 4 ka. After ~4 ka, a sharp decrease in forest cover (from ~40% to ~20%) is
306 observed, corresponding to a 50% decline of tree cover.

307

308 **4 Discussion**

309

310 **4.1 REVEALS model performance in western Tasmania**

311 REVEALS corrects for dispersal and productivity biases in pollen data, hence the choice of the
312 dispersal model alters the reconstructions. Application of REVEALS-GPM and REVEALS-LSM produced
313 considerably better results than the raw percentages of key pollen taxa (Fig. 3, Fig.4). The PCA biplot
314 (Fig. 3) shows the LSM outperformed the more commonly used GPM. Improvement is more evident
315 for Dove Lake, likely due to its small size (~90 ha) relative to Lake St. Clair (4500 ha). REVEALS-LSM
316 results for unstable and windy unstable conditions are very consistent, whereas REVEALS-GPM
317 results are more sensitive to wind parameters (Fig. 3). REVEALS-LSM estimates for Dove Lake are

318 close to actual plant cover, and, thus, appear realistic. REVEALS-GPM performs similarly with high
319 wind speed, however, PPEs calculated with the GPM are unrealistic (Mariani *et al.*, 2016). Our results
320 suggest that LSM is a better model for pollen dispersal and deposition in western Tasmania.

321

322 Pollen dispersal over long distances - the most important for pollen deposition in larger lakes - is
323 mainly carried by turbulent flows and updrafts (Jackson & Lyford, 1999). GPMs do not describe such
324 asymmetric airflows and therefore appear only suited to predict short-distance dispersal
325 (Theuerkauf *et al.*, 2016). The Lagrangian stochastic model simulates updrafts and may be more
326 suitable to model pollen deposition in lakes (Theuerkauf *et al.*, 2013). Updraft velocities are typically
327 much higher than the fall speed of pollen, which explains the greater difference between estimates
328 produced by REVEALS-GPM and REVEALS-LSM for taxa characterized by very large pollen grains,
329 such as *N. cunninghamii* and *G. sphaerocephalus* (Fig.S7 and S8).

330

331 We conclude that the REVEALS model can be successfully applied to Holocene fossil pollen records in
332 western Tasmania. This represents an important advance in Southern Hemisphere palaeoecology
333 and for systems in which animal-pollination is common. A critical limitation of model application in
334 our study region is the scarcity of large (>1 km²) natural lakes. However, model applicability can be
335 tested by substituting single large lakes with multiple small sites, as proposed in southern Sweden
336 (Trondman *et al.*, 2015) or using other simulation-based reconstruction approaches (Bunting &
337 Middleton, 2009; Mrotzek *et al.*, 2017).

338

339 **4.2 Holocene land cover changes in western Tasmania**

340

341 Our land cover estimates reveal a landscape dominated by open vegetation through the entire
342 Holocene (Fig. 5). Early Holocene forest cover was approximately 40%, increasing towards a rain
343 forest maximum in the mid-Holocene, a period when forest and non-forest equally shared 50% of
344 the landscape. This vegetation mix corresponds with peak rain forest pollen content in pollen
345 records from western Tasmania (e.g. Macphail, 1979; Markgraf *et al.*, 1986; Colhoun, 1996a;
346 Fletcher & Moreno, 2012) and a minimum in regional fire activity (Fig. 5; Fletcher and Moreno, 2012;
347 Fletcher *et al.*, 2015). This period is synchronous with a phase (9.2 - 5 ka) of surplus moisture
348 promoting speleothem growth in Lynds Cave (Xia *et al.*, 2001), approximately 25 km NNW of Dove
349 Lake. Wetter conditions in Tasmania during this phase are linked to an enhancement and/or
350 northward-displacement of the prevailing mid-latitude Southern Westerly Winds (SWW) (Fletcher &
351 Moreno, 2011; 2012), which drove lake level fluctuations in southern Australia and hydroclimatic

352 change across the Southern Hemisphere mid-latitudes (Fletcher & Moreno, 2012; Wilkins *et al.*,
353 2013).

354

355 A late-Holocene rain forest decline around Dove Lake occurred in response to decreased moisture
356 availability and a concomitant increase in fire activity across western Tasmania (Fletcher and
357 Moreno, 2012; Fletcher *et al.*, 2014, 2015; Rees *et al.*, 2015; Beck *et al.*, 2017). These changes are
358 linked to increasingly frequent El Niño events in the tropical Pacific (McGlone *et al.*, 1992; Moy *et al.*,
359 2002; Donders *et al.*, 2008), which are associated with drier conditions and increased fire activity in
360 south-east Australia today (Nicholls & Lucas, 2007; Mariani & Fletcher, 2016b). The sharp decline in
361 forest cover at 4.1 ± 0.1 ka is, considering age uncertainties, virtually synchronous with an increase
362 in fire activity observed across western Tasmania at 4.0 ka (Fletcher, *et al.*, 2015; Fig. 5e). While it is
363 impossible to distinguish between anthropogenic and climatic drivers of this fire activity, historical
364 ignitions in Tasmania are almost entirely of human origin (Bowman and Brown, 1986). The long
365 occupation (>35 kyrs) and people's historically documented use of fire to manage landscapes
366 (Plomley, 1966; Thomas, 1995b) argues strongly for a climatically-modulated fire regime in which
367 humans were the primary ignition source.

368

369 Comparison with another record from a small site (0.51 ha) near Dove Lake, Wombat Pool (~1.5 km
370 north-west of Dove Lake) (Stahle *et al.*, 2016) offers insights into local fire and vegetation dynamics.
371 A peak in macroscopic charcoal is recorded at Wombat Pool and Dove Lake at 3.7 ka, indicating
372 enhanced local fire activity. Paradoxically, this peak in local fire activity occurs after the main
373 vegetation change around Dove Lake (Fig. 5). Regional vegetation change therefore occurred prior
374 the local increase in fire activity surrounding Dove Lake, likely in response to regional hydroclimatic
375 and fire regime change. The close match between regional vegetation shifts at Dove Lake and
376 regional charcoal influx from western Tasmania (Fig. 5e) suggests the Dove Lake land cover record
377 reflects climate-vegetation dynamics that were mediated by humans and fire activity.

378

379 **4.3. Did moorland dominate Holocene landscapes of western Tasmania?**

380

381 Our land-cover estimates prove the persistence of treeless vegetation through the entire Holocene,
382 with *G. sphaerocephalus* accounting for 15-45% (REVEALS-LSM) of land cover throughout the
383 reconstruction period (Fig. 5). Pollen percentages for this taxon vary between 2 and 8% (Fig. 2),
384 highlighting severe under-representation (Fletcher & Thomas, 2007). Tasmanian moorland
385 vegetation, although dominated by *G. sphaerocephalus* (Jarman *et al.*, 1988), includes other taxa,

386 including *Leptospermum*, Poaceae, Restionaceae, *Melaleuca*, *Sprengelia* and *Gleichenia* (Jarman,
387 1988). Most of these are also found within other vegetation formations (e.g. heath, *Eucalyptus*
388 woodlands, sclerophyll forests), making them less reliable indicators of moorland. Hence, our
389 moorland abundance reconstructions based on *G. sphaerocephalus* must be considered as absolute
390 minimum values for western Tasmania moorlands. Other approaches, such as the Multiple Scenario
391 Approach (Bunting & Middleton, 2009), should be implemented in future to test the possible range
392 of abundances of these communities.

393

394 The landscape-scale decoupling of vegetation and climate in western Tasmania has intrigued
395 ecologists and archaeologists for decades (Jackson, 1968; Thomas, 1993, 1995a,b; Cosgrove, 1995;
396 Colhoun, 1996; Fletcher and Thomas, 2007; 2010; Macphail, 2010; Colhoun and Shimeld, 2012). We
397 find no evidence for rain forest (the climatic climax vegetation) dominance in the landscape at any
398 time through the Holocene around Dove Lake, enabling us to reject models that invoke late
399 Holocene replacement of a rain forest-dominated landscape by moorland (Macphail, 1979; Colhoun,
400 1996). Instead, we support the inheritance of Late Pleistocene landscape openness through the
401 Holocene to the present (Fletcher & Thomas, 2010a). This model contends that the people's arrival
402 to a largely treeless landscape during the Last Glacial Cycle (ca. 35 ka) and their subsequent
403 manipulation of fire regimes restricted Holocene expansion of typical interglacial vegetation (i.e. rain
404 forest) (Colhoun & van der Geer, 1998) to areas protected from fire. Instead, plants tolerant of
405 frequent burning and an interglacial climate (i.e. moorland and associated sclerophyllous species)
406 expanded at the Pleistocene—Holocene transition and remained dominant through the Holocene.
407 Indeed, *G. sphaerocephalus* is absent from pre-Holocene interglacial pollen spectra (Colhoun and
408 van der Geer, 1998; Colhoun *et al.*, 1999), and Holocene sequences have significantly more charcoal
409 than pre-Holocene interglacials (Fletcher and Thomas, 2010a). Thus, we provide empirical support
410 for the Late Pleistocene inheritance model and the notion that western Tasmania constitutes an
411 ancient cultural landscape (Fletcher and Thomas, 2010a).

412

413 **5 Conclusion**

414 Statistical analysis of modern pollen and plant cover estimates in western Tasmania shows a more
415 realistic performance of REVEALS estimates based on the Lagrangian stochastic model (LSM) when
416 compared to widely-used Gaussian plume model. REVEALS-LSM effectively corrects for biases of
417 productivity and dispersal, allowing better quantification of palynologically-underrepresented plant
418 taxa. Our reconstruction quantifies change in landscape openness in a defined geographic area for
419 the first time in the Southern Hemisphere. Results indicate a landscape dominated by treeless

420 vegetation throughout the last 12 kyrs. We identify a regional shift in regional vegetation at ca. 4 ka,
421 manifest as a rapid halving of rain forest cover from 40% to 20% landscape cover. This phase likely
422 reflects a modulation of the effects of regional-scale anthropogenic burning in response to regional
423 climatic change. Finally, evidence for a persistently open landscape supports the notion that this
424 region represents an ancient cultural landscape resulting from the influence of anthropogenic
425 burning through the last glacial cycle and its influence over post-glacial vegetation development.

426

427 **Acknowledgements**

428 Research was supported by Australian Research Council grants DI110100019 and IN140100050 and
429 an AINSE AWARD (ALNGRA16024). MM was also supported by an AINSE PGRA scholarship (#12039)
430 and the John and Allan Gilmour Science Award (Faculty of Science, University of Melbourne). We
431 acknowledge that our work was conducted on Tasmanian Aboriginal lands and thank the Tasmanian
432 Aboriginal community for their support. We thank Michael Comfort from the Department of Primary
433 Industries, Parks, Water & Environment (DPIPWE) for granting the permit to core Dove Lake. Thanks
434 to Felicitas Hopf for providing surface sample pollen data for Lake St. Clair, and to Kristen Beck,
435 Valentina Vanghi, Anthony Romano and Coralie Tate for assistance in the field.

436

437 **REFERENCES**

- 438 Abraham, V. & Kozáková, R. (2012) Relative pollen productivity estimates in the modern agricultural
439 landscape of Central Bohemia (Czech Republic). *Review of Palaeobotany and Palynology*,
440 **179**, 1-12.
- 441 Anderson, N.J., Bugmann, H., Dearing, J.A. & Gaillard, M.-J. (2006) Linking palaeoenvironmental data
442 and models to understand the past and to predict the future. *Trends in Ecology & Evolution*,
443 **21**, 696-704.
- 444 Beck, K.K., Fletcher, M.-S., Gadd, P., Heijnis, H. & Jacobsen, G. (2017) An early onset of ENSO
445 influence in the extra-tropics of the southwest Pacific inferred from a 14, 600 year high
446 resolution multi-proxy record from Paddy's Lake, northwest Tasmania. *Quaternary Science*
447 *Reviews*, **157**, 164-175..
- 448 Birks, J.B., Lotter, A.F., Juggins, S. & Smol, J.P. (2012) *Tracking environmental change using lake*
449 *sediments: data handling and numerical techniques*. Springer, Dordrecht.
- 450 Bond, W.J., Woodward, F.I. & Midgley, G.F. (2005) The global distribution of ecosystems in a world
451 without fire. *New Phytologist*, **165**, 525-537.

- 452 Bowman, D. & Brown, M. (1986) Bushfires in Tasmania: a botanical approach to anthropological
453 questions. *Archaeology in Oceania*, **21**, 166-171.
- 454 Bowman, D.M. (1998) The impact of Aboriginal landscape burning on the Australian biota. *New*
455 *Phytologist*, **140**, 385-410.
- 456 Bowman, D.M.J.S. (2000) *Australian rainforests: islands of green in a land of fire*, First edn.
457 Cambridge University Press, Cambridge.
- 458 Bowman, D.M.J.S. & Jackson, W.D. (1981) Vegetation succession in southwest Tasmania. *Search*, **12**,
459 358-362.
- 460 Bradstock, R.A., Williams, J.E. & Gill, M.A. (2002) *Flammable Australia: the fire regimes and*
461 *biodiversity of a continent*. Cambridge University Press.
- 462 Brown, M.J. & Podger, F.D. (1982a) Floristics and fire regimes of a vegetation sequence from
463 sedgeland-heath to rainforest at Bathurst Harbour, Tasmania. *Australian Journal of Botany*,
464 **30**, 659-676.
- 465 Brown, M.J. & Podger, F. (1982b) On the apparent anomaly between observed and predicted
466 percentages of vegetation types in south-west Tasmania. *Australian Journal of Ecology*, **7**,
467 203-295.
- 468 Bunting, M. & Middleton, R. (2009) Equifinality and uncertainty in the interpretation of pollen data:
469 the Multiple Scenario Approach to reconstruction of past vegetation mosaics. *The Holocene*,
470 **19**, 799-803.
- 471 Colhoun, E.A. (1996a) Application of Iversen's glacial-interglacial cycle to interpretation of the Last
472 Glacial and Holocene vegetation of western Tasmania. *Quaternary Science Reviews*, **15**, 557-
473 580.
- 474 Colhoun, E.A. (1996b) Application of Iversen's glacial-interglacial cycle to interpretation of the late
475 last glacial and Holocene vegetation history of western Tasmania. *Quaternary Science*
476 *Reviews*, **15**, 557-580.
- 477 Colhoun, E.A. & van der Geer, G. (1998) Pollen analysis of 0-20m at Darwin Crater, western
478 Tasmania, Australia. *International Project of Paleolimnology and Late Cenozoic Climate*, **11**,
479 68-89.
- 480 Colhoun, E.A., Pola, J.S., Barton, C.E. & Heijnis, H. (1999) Late Pleistocene vegetation and climate
481 history of Lake Selina, western Tasmania. *Quaternary International*, **57-58**, 5-23.
- 482 Colhoun, E.A. & Shimeld, P.W. (2012) Late-Quaternary vegetation history of Tasmania from pollen
483 records. *Peopled Landscapes: Archaeological and Biogeographic Approaches to Landscapes*.
484 *Terra Australis*, **34**, 29.

- 485 Cosgrove, R. (1995) Late Pleistocene behavioral variation and time trends: the case from Tasmania.
486 *Archaeology in Oceania*, **30**, 83 - 104.
- 487 Cosgrove, R. (1999) Forty-two degrees south: the archaeology of Late Pleistocene Tasmania. *Journal*
488 *of World Prehistory*, **13**, 357-402.
- 489 de Nascimento, L., Nogué, S., Fernández-Lugo, S., Méndez, J., Otto, R., Whittaker, R.J., Willis, K.J. &
490 Fernández-Palacios, J.M. (2015) Modern pollen rain in Canary Island ecosystems and its
491 implications for the interpretation of fossil records. *Review of Palaeobotany and Palynology*,
492 **214**, 27-39.
- 493 Dearing, J.A., Braimoh, A.K., Reenberg, A., Turner, B.L. & van der Leeuw, S. (2010) Complex land
494 systems: the need for long time perspectives to assess their future. *Ecology and Society*, **15**,
495 21.
- 496 Donders, T.H., Wagner-Cremer, F. & Visscher, H. (2008) Integration of proxy data and model
497 scenarios for the mid-Holocene onset of modern ENSO variability. *Quaternary Science*
498 *Reviews*, **27**, 571-579.
- 499 Donders, T.H., Haberle, S., Hope, G., Wagner, F. & Visscher, H. (2007) Pollen evidence for the
500 transition of the Eastern Australian climate system from the post-glacial to the present-day
501 ENSO mode. *Quaternary Science Reviews*, **26**, 1621-1637.
- 502 Faegri, K. & Iversen, J. (1989) *Textbook of pollen analysis*. Wiley, New York.
- 503 Fletcher, M.-S. & Thomas, I. (2007a) Holocene vegetation and climate change from near Lake
504 Pedder, south-west Tasmania, Australia. *Journal of Biogeography*, **34**, 665-677.
- 505 Fletcher, M.-S. & Thomas, I. (2007b) Modern pollen–vegetation relationships in western Tasmania,
506 Australia. *Review of Palaeobotany and Palynology*, **146**, 146-168.
- 507 Fletcher, M.-S. & Thomas, I. (2010a) The origin and temporal development of an ancient cultural
508 landscape. *Journal of Biogeography*, **37**, 2183–2196.
- 509 Fletcher, M.-S. & Thomas, I. (2010b) A Holocene record of sea level, vegetation, people and fire from
510 western Tasmania, Australia. *The Holocene*, **20**, 351-361.
- 511 Fletcher, M.-S. & Moreno, P.I. (2011) Zonally symmetric changes in the strength and position of the
512 Southern Westerlies drove atmospheric CO₂ variations over the past 14 k.y. *Geology*, **39**,
513 419-422.
- 514 Fletcher, M.-S. & Moreno, P.I. (2012) Have the Southern Westerlies changed in a zonally symmetric
515 manner over the last 14,000 years? A hemisphere-wide take on a controversial problem.
516 *Quaternary International*, **253**, 32–46.
- 517 Fletcher, M.-S., Wood, S.W. & Haberle, S.G. (2014a) A fire-driven shift from forest to non-forest:
518 evidence for alternative stable states? *Ecology*, **95**, 2504-2513.

- 519 Fletcher, M.-S., Benson, A., Heijnis, H., Gadd, P.S., Cwynar, L.C. & Rees, A.B.H. (2015) Changes in
520 biomass burning mark the onset an ENSO-influenced climate regime at 42°S in southwest
521 Tasmania, Australia. *Quaternary Science Reviews*, **122**, 222-232.
- 522 Fletcher, M.-S., Wolfe, B.B., Whitlock, C., Pompeani, D.P., Heijnis, H., Haberle, S.G., Gadd, P.S. &
523 Bowman, D.M.J.S. (2014b) The legacy of mid-Holocene fire on a Tasmanian montane
524 landscape. *Journal of Biogeography*, **41**, 476-488.
- 525 Foley, J.A., Costa, M.H., Delire, C., Ramankutty, N. & Snyder, P. (2003) Green surprise? How
526 terrestrial ecosystems could affect earth's climate. *Frontiers in Ecology and the Environment*,
527 **1**, 38-44.
- 528 Gaillard, M.-J., Birks, H.J.B., Ihse, M. & Runborg, S. (1998) Pollen/landscape calibrations based on
529 modern pollen assemblages from surface-sediment samples and landscape mapping-a pilot
530 study in South Sweden. *Palaeoclimate Research*, **27**, 31-52.
- 531 Gaillard, M.-J., Sugita, S., Mazier, F., Trondman, A.-K., Brostrom, A., Hickler, T., Kaplan, J.O.,
532 Kjellström, E., Kokfelt, U. & Kunes, P. (2010) Holocene land-cover reconstructions for studies
533 on land cover-climate feedbacks. *Climate of the Past*, **6**, 483-499.
- 534 Gentili, J. (1972) *Australian climate patterns*. The Griffin Press, Adelaide.
- 535 Hellman, S., Gaillard, M.J., Broström, A. & Sugita, S. (2008) The REVEALS model, a new tool to
536 estimate past regional plant abundance from pollen data in large lakes: validation in
537 southern Sweden. *Journal of Quaternary Science*, **23**, 21-42.
- 538 Hopf, F.V.L., Colhoun, E.A. & Barton, C.E. (2000) Late-glacial and Holocene record of vegetation and
539 climate from Cynthia bay, Lake StClair, Tasmania. *Journal of Quaternary Science*, **15**, 725-
540 732.
- 541 Hultberg, T., Gaillard, M.-J., Grundmann, B. & Lindbladh, M. (2015) Reconstruction of past landscape
542 openness using the Landscape Reconstruction Algorithm (LRA) applied on three local pollen
543 sites in a southern Swedish biodiversity hotspot. *Vegetation History and Archaeobotany*, **24**,
544 253-266.
- 545 Jackson, S.T. & Lyford, M.E. (1999) Pollen dispersal models in Quaternary plant ecology:
546 assumptions, parameters, and prescriptions. *The Botanical Review*, **65**, 39-75.
- 547 Jackson, W.D. (1968) Fire, air, water and earth – an elemental ecology of Tasmania. *Proceedings of*
548 *the Ecological Society of Australia*, **3**, 9-16.
- 549 Jacobson, G.L. & Bradshaw, R.H.W. (1981) The selection of sites for paleovegetational studies.
550 *Quaternary Research*, **16**, 80-96.
- 551 Jarman, S.J., Kantivalis, G. & Brown, M.J. (1988) *Buttongrass moorlands in Tasmania*. *Tasmanian*
552 *Forest Research Council Research Report No. 3*. Tasmanian Forest Research Council, Hobart.

553 Jolliffe, I. (2002) *Principal component analysis*. Wiley Online Library.

554 Kaplan, J.O., Prentice, I.C., Knorr, W. & Valdes, P.J. (2002) Modeling the dynamics of terrestrial
555 carbon storage since the Last Glacial Maximum. *Geophysical Research Letters*, **29**, 22

556 Kirkpatrick, J.A. & Dickinson, K.J.M. (1984) The impact of fire on Tasmanian vegetation and soils.
557 *Australian Journal of Botany*, **32**, 613-629.

558 Kuneš, P., Odgaard, B.V. & Gaillard, M.J. (2011) Soil phosphorus as a control of productivity and
559 openness in temperate interglacial forest ecosystems. *Journal of Biogeography*, **38**, 2150-
560 2164.

561 Kuneš, P., Svobodová-Svitavská, H., Kolář, J., Hajnalová, M., Abraham, V., Macek, M., Tkáč, P. &
562 Szabó, P. (2015) The origin of grasslands in the temperate forest zone of east-central Europe:
563 long-term legacy of climate and human impact. *Quaternary Science Reviews*, **116**, 15-27.

564 Kuparinen, A., Markkanen, T., Riikonen, H. & Vesala, T. (2007) Modeling air-mediated dispersal of
565 spores, pollen and seeds in forested areas. *Ecological modelling*, **208**, 177-188.

566 Macphail, M. (2010) The burning question: Claims and counter claims on the origin and extent of
567 buttongrass moorland (blanket moor) in southwest Tasmania during the present
568 glacialinterglacial. *Terra Australis*, **32**, 323-339.

569 Macphail, M.K. (1979) Vegetation and climates in southern Tasmania since the last glaciation.
570 *Quaternary Research*, **11**, 306-341.

571 Mariani, M. & Fletcher, M.S. (2016) The Southern Annular Mode determines inter-annual and
572 centennial-scale fire activity in temperate southwest Tasmania, Australia. *Geophysical*
573 *Research Letters*, **43**, 1702–1709.

574 Mariani, M., Connor, S., Theuerkauf, M., Kuneš, P. & Fletcher, M.-S. (2016) Testing quantitative
575 pollen dispersal models in animal-pollinated vegetation mosaics: An example from
576 temperate Tasmania, Australia. *Quaternary Science Reviews*, **154**, 214-225.

577 Markgraf, V., Bradbury, J.P. & Busby, J.R. (1986) Palaeoclimates in southwestern Tasmania during
578 the last 13,000 years. *Palios*, **1**, 368-380.

579 Mazier, F., Gaillard, M.-J., Kuneš, P., Sugita, S., Trondman, A.-K. & Broström, A. (2012) Testing the
580 effect of site selection and parameter setting on REVEALS-model estimates of plant
581 abundance using the Czech Quaternary Palynological Database. *Review of Palaeobotany and*
582 *Palynology*, **187**, 38-49.

583 McCune, B. & Mefford, M.J. (1999) *PC-Ord for Windows*. MjM Software, Gleneden Beach.

584 McGlone, M.S., Kershaw, P. & Markgraf, V. (1992) El Nino/Southern Oscillation climatic variability in
585 Australasian and South American paleoenvironmental records. *El Nino: historical and*

- 586 *paleoclimatic aspects of the southern oscillation* (ed. by H.F. Diaz and V. Markgraf).
587 Cambridge University Press, Cambridge, 435-462.
- 588 Moy, C.M., Seltzer, G.O., Rodbell, D.T. & Anderson, D.M. (2002) Variability of El Nino/Southern
589 Oscillation activity at millennial timescales during the Holocene. *Nature*, **420**, 162-165.
- 590 Nicholls, N. & Lucas, C. (2007) Interannual variations of area burnt in Tasmanian bushfires:
591 relationships with climate and predictability. *International Journal of Wildland Fire*, **16**, 540-
592 546.
- 593 Oksanen, J., Kindt, R., Legendre, P., O'Hara, B., Stevens, M., Oksanen, M. & Suggests, M. (2015)
594 Vegan community ecology package: ordination methods, diversity analysis and other
595 functions for community and vegetation ecologists. Version 2.3-1.
- 596 Plomley, N.J.B. (1966) *Friendly Mission: The Tasmanian Journals and Papers of George Augustus*
597 *Robinson 1829-1834* (Kingsgrove: Tasmanian Historical Research Association).
- 598 Prentice, I.C. (1985) Pollen Representation, Source Area, and Basin Size: Toward a Unified Theory of
599 Pollen Analysis. *Quaternary Research*, **23**, 76-86.
- 600 Sitch, S., Smith, B., Prentice, I.C., Arneeth, A., Bondeau, A., Cramer, W., Kaplan, J., Levis, S., Lucht, W.
601 & Sykes, M.T. (2003) Evaluation of ecosystem dynamics, plant geography and terrestrial
602 carbon cycling in the LPJ dynamic global vegetation model. *Global Change Biology*, **9**, 161-
603 185.
- 604 Smith, B., Samuelsson, P., Wramneby, A. & Rummukainen, M. (2011) A model of the coupled
605 dynamics of climate, vegetation and terrestrial ecosystem biogeochemistry for regional
606 applications. *Tellus A*, **63**, 87-106.
- 607 Stahle, L.N., Whitlock, C. & Haberle, S.G. (2016) A 17,000-year-long record of vegetation and fire
608 from Cradle Mountain National Park, Tasmania. *Frontiers in Ecology and Evolution*, **4**, 82.
- 609 Strandberg, G., Kjellström, E., Poska, A., Wagner, S., Gaillard, M.-J., Trondman, A.-K., Mauri, A.,
610 Kaplan, J., Birks, H. & Bjune, A. (2014) Regional climate model simulations for Europe at 6
611 and 0.2 k BP: sensitivity to changes in anthropogenic deforestation. *Climate of the Past*, **10**,
612 661-680.
- 613 Sturman, A.P. & Tapper, N.J. (2006) *The weather and climate of Australia and New Zealand*. Oxford
614 University Press.
- 615 Sugita, S. (1993) A model of pollen source area for an entire lake surface. *Quaternary Research*, **39**,
616 239-244.
- 617 Sugita, S. (1994) Pollen representation of vegetation in Quaternary sediments: theory and method in
618 patchy vegetation. *Journal of Ecology*, **1**, 881-897.

- 619 Sugita, S. (2007a) Theory of quantitative reconstruction of vegetation II: all you need is LOVE. *The*
620 *Holocene*, **17**, 243-257.
- 621 Sugita, S. (2007b) Theory of quantitative reconstruction of vegetation I: pollen from large sites
622 REVEALS regional vegetation composition. *The Holocene*, **17**, 229-241.
- 623 Sugita, S., Gaillard, M.-J. & Brostrom, A. (1999) Landscape openness and pollen records: a simulation
624 approach. *The Holocene*, **9**, 409-421.
- 625 Sugita, S., Parshall, T., Calcote, R. & Walker, K. (2010) Testing the Landscape Reconstruction
626 Algorithm for spatially explicit reconstruction of vegetation in northern Michigan and
627 Wisconsin. *Quaternary Research*, **74**, 289-300.
- 628 Sutton, O. (1953) *Micrometeorology*. McGraw-Hill, New York
- 629 Theuerkauf, M., Kuparinen, A. & Joosten, H. (2013) Pollen productivity estimates strongly depend on
630 assumed pollen dispersal. *The Holocene*, **23**(1), 14-24
- 631 Theuerkauf, M., Couwenberg, J., Kuparinen, A. & Liebscher, V. (2016) A matter of dispersal:
632 REVEALSinR introduces state-of-the-art dispersal models to quantitative vegetation
633 reconstruction. *Vegetation History and Archaeobotany*, **25**(6), 541-553.
- 634 Thomas, I. (1993) Late Pleistocene Environments and Aboriginal Settlement Patterns in Tasmania.
635 *Australian Archaeology*, **36**, 1-11.
- 636 Thomas, I. (1995a) "Where have all the forests gone?" New pollen evidence from Melaleuca Inlet in
637 Southwestern Tasmania. *IAG 1993 Conference Proceedings* (ed by G. Dixon and D. Aitkin),
638 pp. 295-301. Melbourne.
- 639 Thomas, I. (1995b) *Ethnohistoric sources for the use of fire by Tasmanian Aborigines: a preliminary*
640 *compilation and investigation of the evidence*. Dept. of Geography and Environmental
641 Studies, University of Melbourne.
- 642 Trondman, A.K., Gaillard, M.J., Mazier, F., Sugita, S., Fyfe, R., Nielsen, A.B., Twiddle, C., Barratt, P.,
643 Birks, H.J.B. & Bjune, A.E. (2015) Pollen-based quantitative reconstructions of Holocene
644 regional vegetation cover (plant-functional types and land-cover types) in Europe suitable
645 for climate modelling. *Global change biology*, **21**, 676-697.
- 646 Whitlock, C. & Larsen, C. (2001) Charcoal as a fire proxy. Smol, JP, Birks, HJB and Last, WM (eds.)
647 Tracking environmental change using lake sediments Vol. 3, Terrestrial, algal, and Siliceous
648 Indicators: 75-97. In. Kluwer Academic Publishers
- 649 Wilkins, D., Gouramanis, C., De Deckker, P., Fifield, L.K. & Olley, J. (2013) Holocene lake-level
650 fluctuations in Lakes Keilambete and Gnotuk, southwestern Victoria, Australia. *The*
651 *Holocene*, **23**(6), 784-795..

652 Wood, S.W. & Bowman, D.M.J.S. (2011) Alternative stable states and the role of fire–vegetation–soil
653 feedbacks in the temperate wilderness of southwest Tasmania. *Landscape Ecology*, 1-16.
654 Wood, S.W., Hua, Q. & Bowman, D.M.J.S. (2011a) Fire-patterned vegetation and the development of
655 organic soils in the lowland vegetation mosaics of south-west Tasmania. *Australian Journal*
656 *of Botany*, **59**, 126-136.
657 Xia, Y., Zhao, J. & Collerson, K.D. (2001) Early-Mid Holocene climatic variations in Tasmania,
658 Australia: multi-proxy records in a stalagmite from Lynds Cave. *Earth and Planetary Science*
659 *Letters*, **194**, 177-187.
660 Yospin, G.I., Wood, S.W., Holz, A., Bowman, D.M., Keane, R.E. & Whitlock, C. (2015) Modeling
661 vegetation mosaics in sub-alpine Tasmania under various fire regimes. *Modeling Earth*
662 *Systems and Environment*, **1**, 1-10.

663

664 **SUPPORTING INFORMATION**

665 Additional Supporting Information may be found in the online version of this article:

666

667 Appendix S1. Topography of the study area.

668 Appendix S2. Core extraction and chronology information.

669 Appendix S3. Extended pollen diagram from Dove Lake.

670 Appendix S4. Pollen zones descriptions for Dove Lake.

671 Appendix S5. Further calculations of PPEs.

672 Appendix S6. Further statistics supporting the REVEALS validation.

673 Appendix S7. Additional REVEALS model runs and taxon-specific estimates.

674

675 **DATA ACCESSIBILITY:** Data produced in the present work are available upon request to
676 mmariani@student.unimelb.edu.au

677

678

679 **BIOSKETCH**

680 **Michela Mariani** is interested in reconstructing past climate and vegetation dynamics to uncover
681 present and future scenarios. Her research is especially focused on fire, human and climate-driven
682 changes of terrestrial ecosystems throughout the Holocene and Late Pleistocene in the Southern
683 Hemisphere.

684 Author contributions: M.M. collected and analysed the data and led the manuscript writing; S.E.C.
685 conceived ideas, data analysis support and manuscript editing; M.-S.F. conceived ideas, fieldwork
686 support and manuscript editing; M.T. methodology support and manuscript editing; P.K.
687 methodology support and manuscript editing; J.G. radiocarbon dating support; K.M.S. analytical
688 support and manuscript editing; A.Z. lead-210 dating support.

689

690

691 **Figures list:**

692 **Fig. 1** Location map of the study site (Dove Lake, Tasmania – TAS1507SC2, red star). The green star
693 indicates the validation site (Lake St Clair). Black box represents the vegetation extent reconstructed
694 by the REVEALS model (100 x 100 km). Red (green) circle is the 50 km buffer around Dove Lake (Lake
695 St Clair) used to extract modern plant cover from the TasVeg 3.0 vegetation maps (Government of
696 Tasmania, 2013) for the REVEALS validation process (see Methods). Polygons in the right panel
697 represent vegetation formations. Lake area is shown as shades of blue representing bathymetry in
698 metres.

699 **Table 1** - Table showing fall speeds and pollen productivity estimates for the ten key pollen taxa
700 used for the vegetation reconstruction (data from Mariani *et al.*, 2016). GPM= Gaussian plume
701 model; LSM= Lagrangian stochastic model.

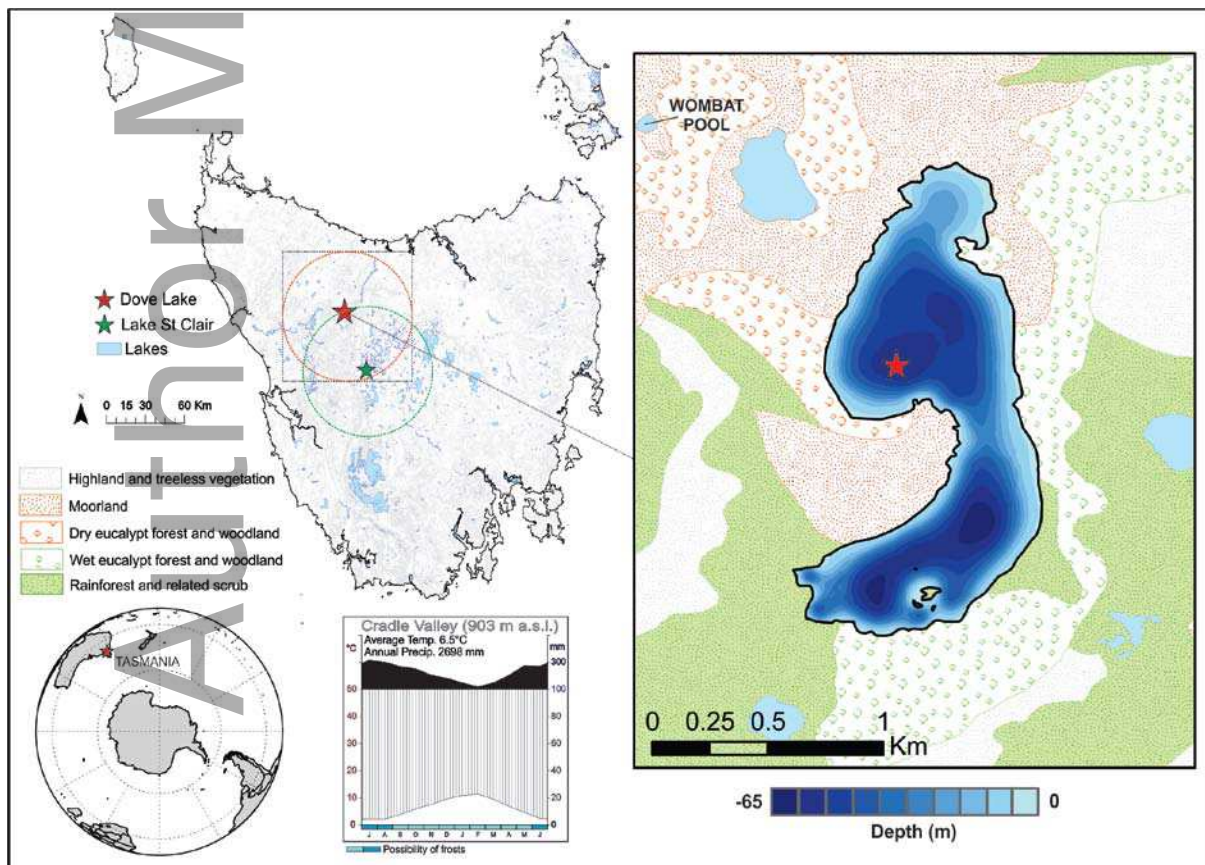
702 **Fig. 2** Diagram showing pollen % of key taxa used for the vegetation reconstruction. Macro- and
703 micro- charcoal accumulation rates (particles/cm² yr⁻¹) are also shown. Colours represent the
704 grouping of the taxa according to vegetation structure: green is used for taxa generally occurring
705 within forests; red is used for plant taxa commonly found in non-forested environments. Dashed
706 lines indicate statistically determined pollen zones (see Appendix S4 for zones' description).

707 **Fig. 3** Plot of the REVEALS validation PCA. REVEALS vegetation estimates from the surface samples of
708 Dove Lake and Lake St. Clair (Tasmania) were compared to the actual modern plant cover around 50
709 km from each lake. REVEALS results from four model runs (REVEALS-GPM3m/s, REVEALS-

710 GPM6.5m/s, REVEALS-LSM and REVEALS-LSM windy) are shown. Axis 1 represents 68.5% of the
 711 variance, whereas Axis 2 represents the 16.5%. Grey arrows highlight taxa with a correlation with
 712 the PCA Axes larger than $r=0.5$. Filled symbols indicate data from Lake St. Clair, hollow symbols
 713 represent Dove Lake. **Fig. 4** Comparison of pollen data and quantitative reconstruction results:
 714 summary diagram showing a) pollen percentages; b) REVEALS vegetation estimates using the
 715 Gaussian plume model (REVEALS-GPM); c) REVEALS vegetation estimates using the Lagrangian
 716 stochastic model (REVEALS-LSM). Dashed lines indicate statistically determined pollen zones (same
 717 as Fig. 2).

718 **Fig. 5** Summary figure showing major palaeoenvironmental trends, including a) reconstructed plant
 719 cover for *Gymnoscheonus sphaerocephalus* (%); b) reconstructed total rainforest cover (%); c)
 720 Reconstructed *Eucalyptus* plant cover; d) Macroscopic CHAR record; e) Fire activity based on
 721 charcoal influx from two alpine sites in western Tasmania (Fletcher et al., 2015). Orange-yellow
 722 shading highlights periods of relatively low moisture, enhanced fire activity and low forest cover.
 723 Green shading identifies the period with maximum forest cover and low fire activity, suggesting
 724 wetter conditions.

725



726

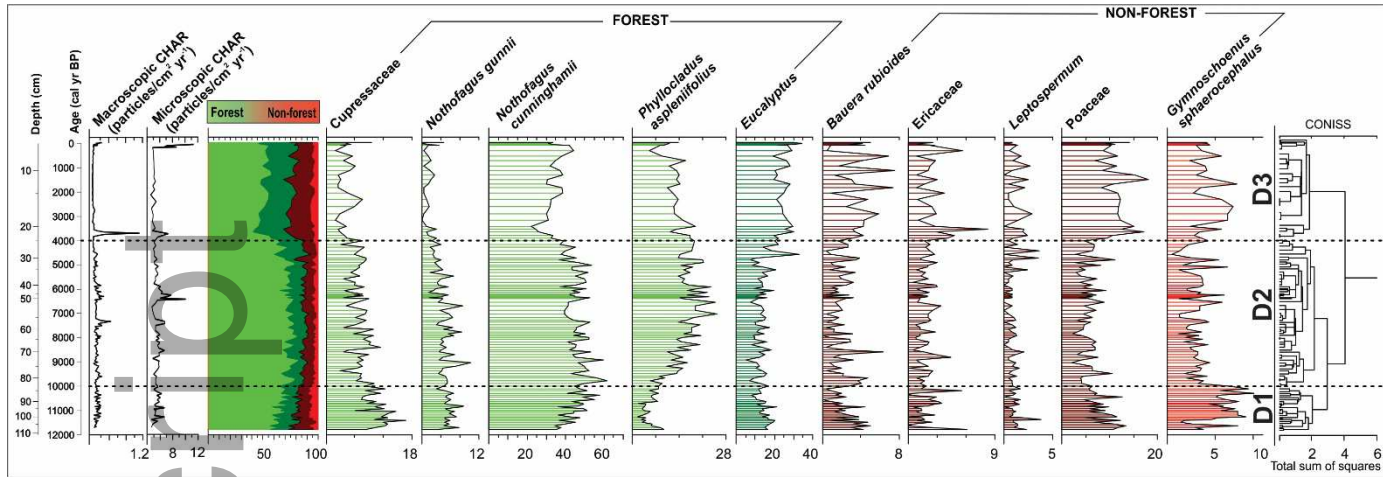
727 **Fig. 1** Location map of the study site (Dove Lake, Tasmania – TAS1507SC2, red star). The green star
 728 indicates the validation site (Lake St Clair). Black box represents the vegetation extent reconstructed
 729 by the REVEALS model (100 x 100 km). Red (green) circle is the 50 km buffer around Dove Lake (Lake
 730 St Clair) used to extract modern plant cover from the TasVeg 3.0 vegetation maps (Government of
 731 Tasmania, 2013) for the REVEALS validation process (see Methods). Polygons in the right panel
 732 represent vegetation formations. Lake area is shown as shades of blue representing bathymetry in
 733 metres.

734
 735

736 **Table 1** - Table showing fall speeds and PPEs for the ten key pollen taxa used for the vegetation
 737 reconstruction from Dove Lake (data from Mariani *et al.*, 2016). GPM= Gaussian plume model; LSM=
 738 Lagrangian stochastic model. Superscripts *f* and *nf* are used to differentiate forest and non-forest
 739 plant taxa.

	Fall speed (m/s)	GPM 10km	GPM 10km SD	LSM 10km	LSM 10km SD
<i>Bauera rubioides</i> ^{nf}	0.004	0.165	0.025	0.067	0.011
Cupressaceae ^f	0.031	1.003	0.124	1.337	0.198
Ericaceae ^{nf}	0.043	0.043	0.004	0.067	0.007
<i>Eucalyptus</i> spp. ^f	0.008	1.000	0.000	1.000	0.000
<i>Gymnoschoenus sphaerocephalus</i> ^{nf}	0.072	0.027	0.003	0.050	0.006
<i>Leptospermum</i> spp. ^{nf}	0.005	0.284	0.027	0.145	0.016
<i>Nothofagus cunninghamii</i> ^f	0.037	0.830	0.055	1.281	0.084
<i>Nothofagus gunnii</i> ^f	0.020	0.251	0.029	0.385	0.033
<i>Phyllocladus aspleniifolius</i> ^f	0.026	0.631	0.099	0.842	0.163
Poaceae ^{nf}	0.030	0.242	0.019	0.414	0.031

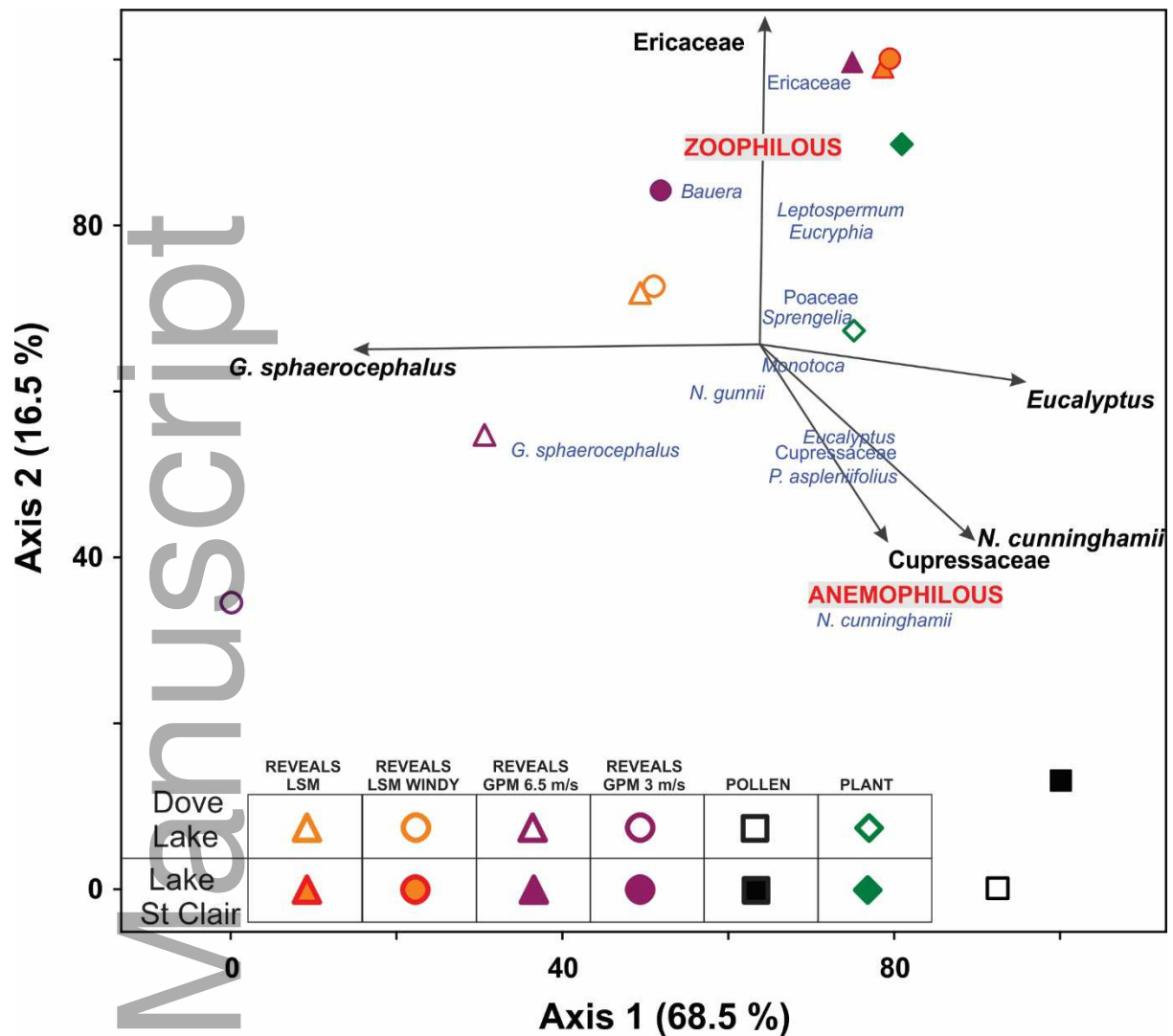
740
 741
 742



743

744 **Fig. 2** Diagram showing pollen % of key taxa used for the vegetation reconstruction. Macro- and
 745 micro- charcoal accumulation rates (particles/cm² yr⁻¹) are also shown. Colours represent the
 746 grouping of the taxa according to vegetation structure: green is used for taxa generally occurring
 747 within forests; red is used for plant taxa commonly found in non-forested environments. Dashed
 748 lines indicate statistically determined pollen zones (see Appendix S4 for zones' description).

749

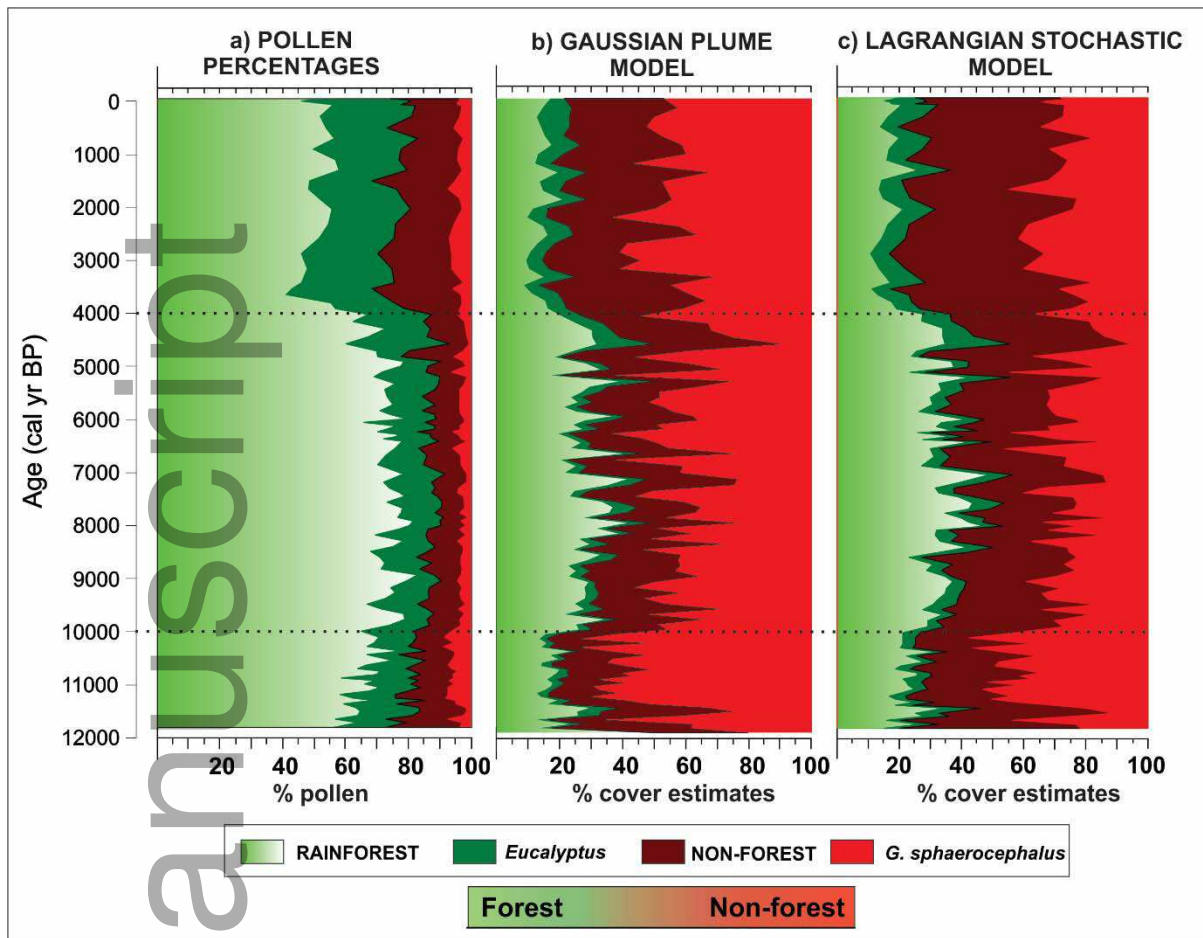


750

751 **Fig. 3** Plot of the REVEALS validation PCA. REVEALS vegetation estimates from the surface samples of
 752 Dove Lake and Lake St. Clair (Tasmania) were compared to the actual modern plant cover around 50
 753 km from each lake. REVEALS results from four model runs (REVEALS-GPM3m/s, REVEALS-
 754 GPM6.5m/s, REVEALS-LSM and REVEALS-LSM windy) are shown. Axis 1 represents 68.5% of the
 755 variance, whereas Axis 2 represents the 16.5%. Grey arrows highlight taxa with a correlation with
 756 the PCA Axes larger than $r=0.5$. Filled symbols indicate data from Lake St. Clair, hollow symbols
 757 represent Dove Lake.

758

759

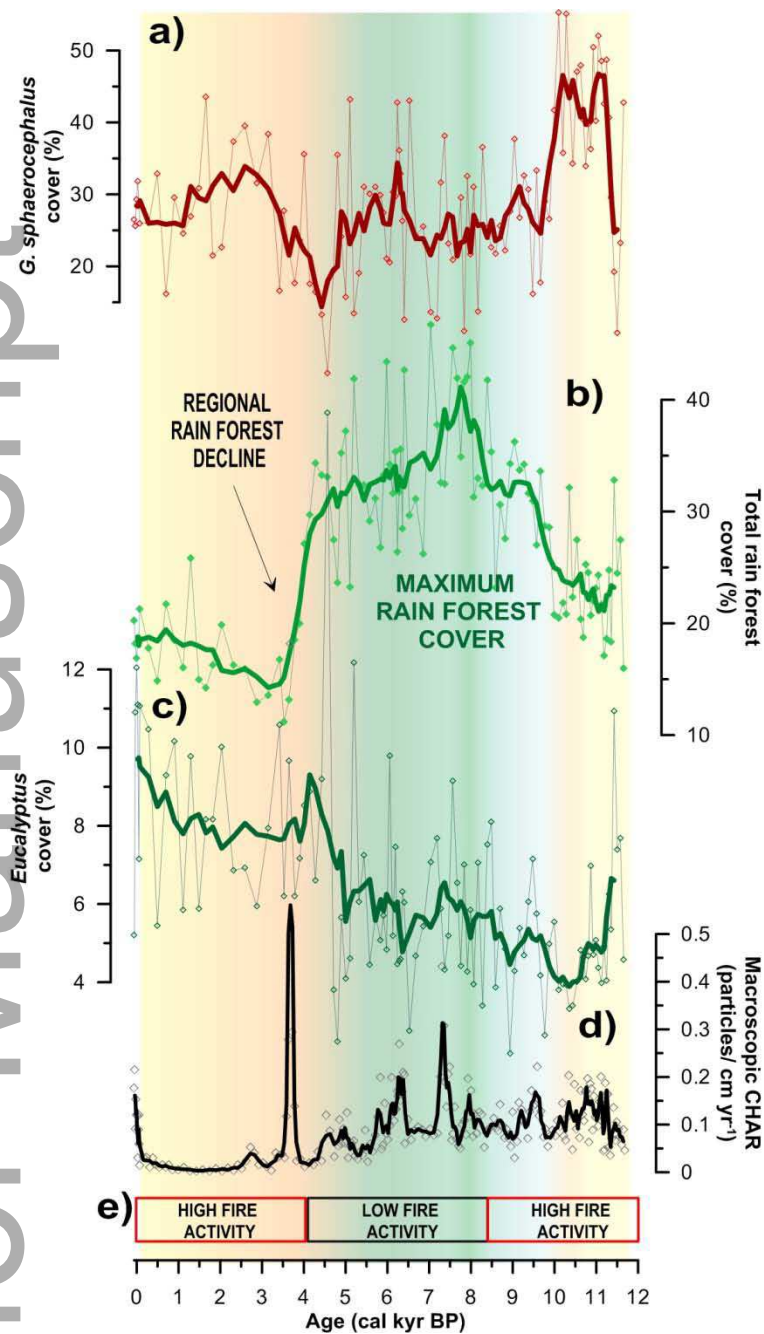


760

761 **Fig. 4** Comparison of pollen data and quantitative reconstruction results: summary diagram showing
 762 a) pollen percentages; b) REVEALS vegetation estimates using the Gaussian plume model under
 763 neutral conditions (REVEALS-GPM); c) REVEALS vegetation estimates using the Lagrangian stochastic
 764 model (REVEALS-LSM). Dashed lines indicate statistically determined pollen zones (same as Fig. 2).

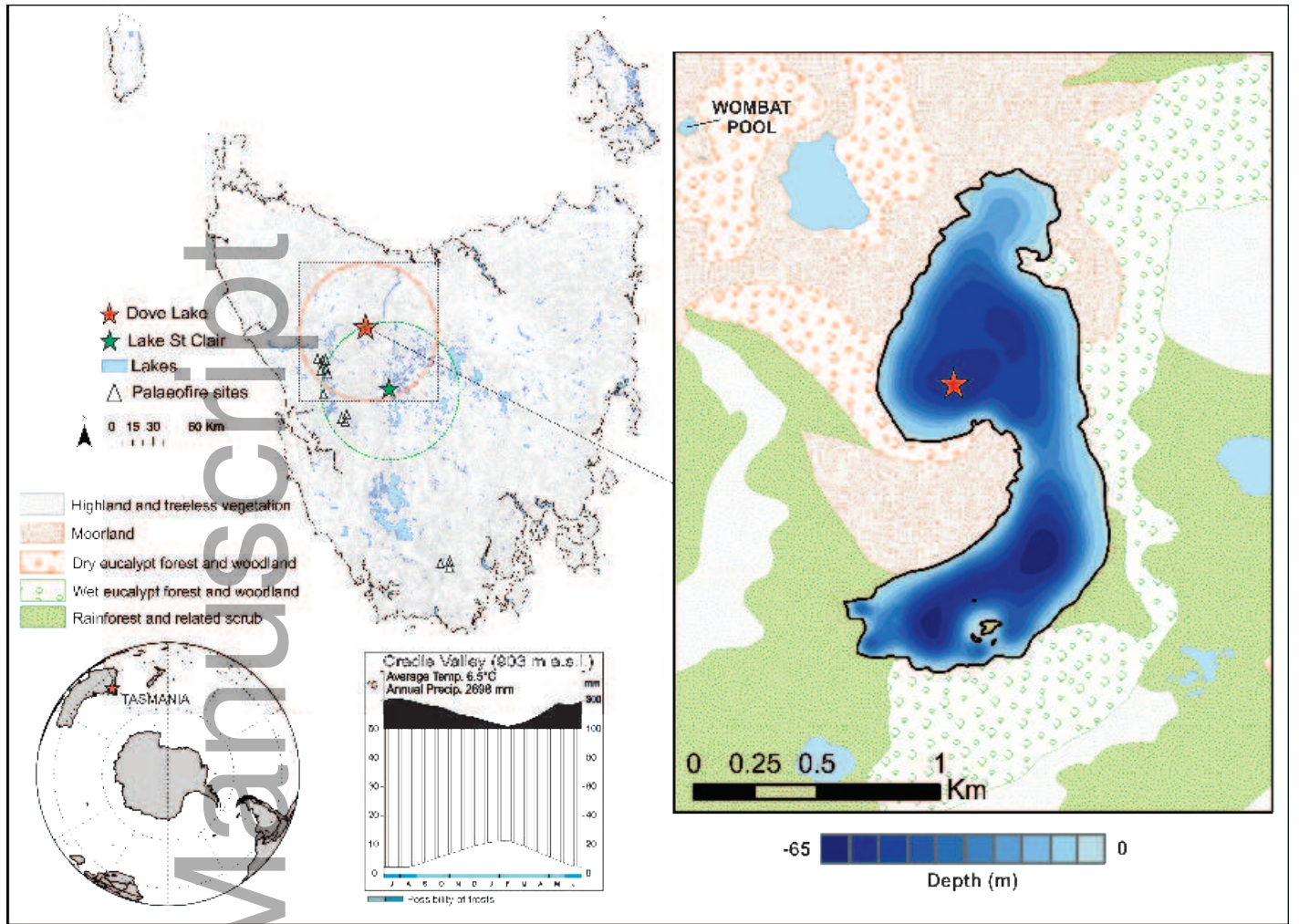
765

766

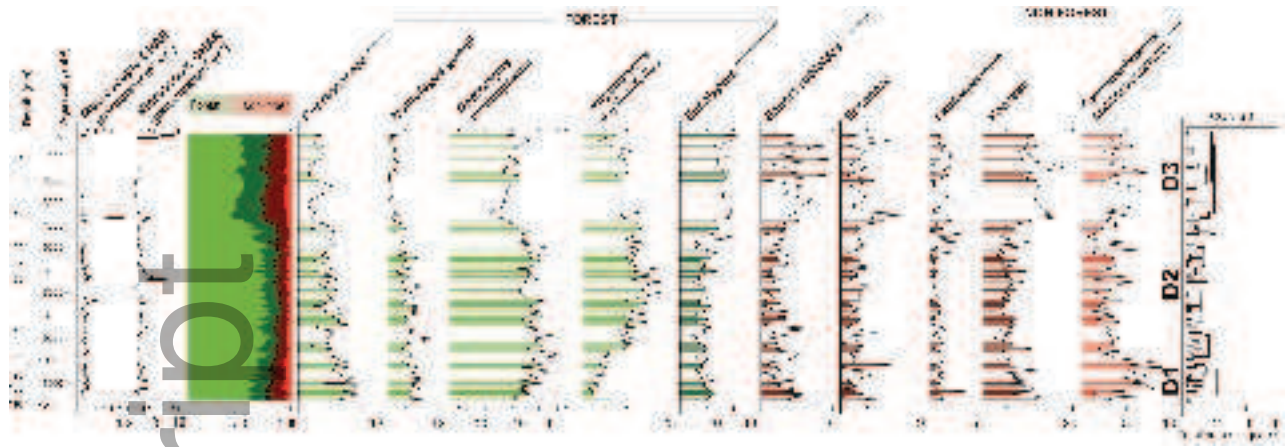


767

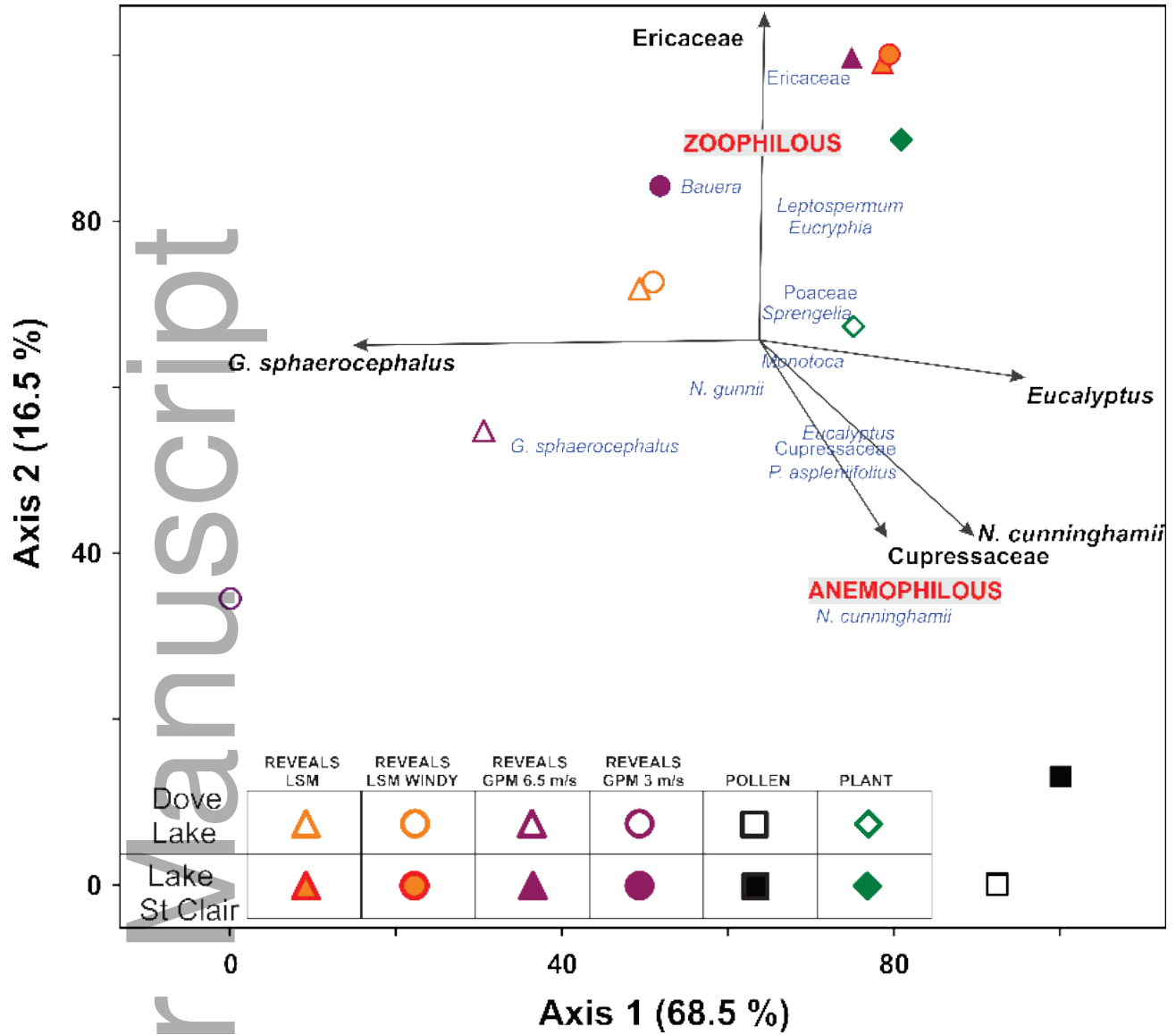
768 **Fig. 5** – Summary figure showing major palaeoenvironmental trends, including a) reconstructed plant
 769 cover for *Gymnoscheonus sphaerocephalus* (%); b) reconstructed total rainforest cover (%); c)
 770 Reconstructed *Eucalyptus* plant cover; d) Macroscopic CHAR record; e) Fire activity based on
 771 charcoal influx from two alpine sites in western Tasmania (Fletcher *et al.*, 2015). Orange-yellow
 772 shading highlights periods of relatively low moisture, enhanced fire activity and low forest cover.
 773 Green shading identifies the period with maximum forest cover and low fire activity, suggesting
 774 wetter conditions.



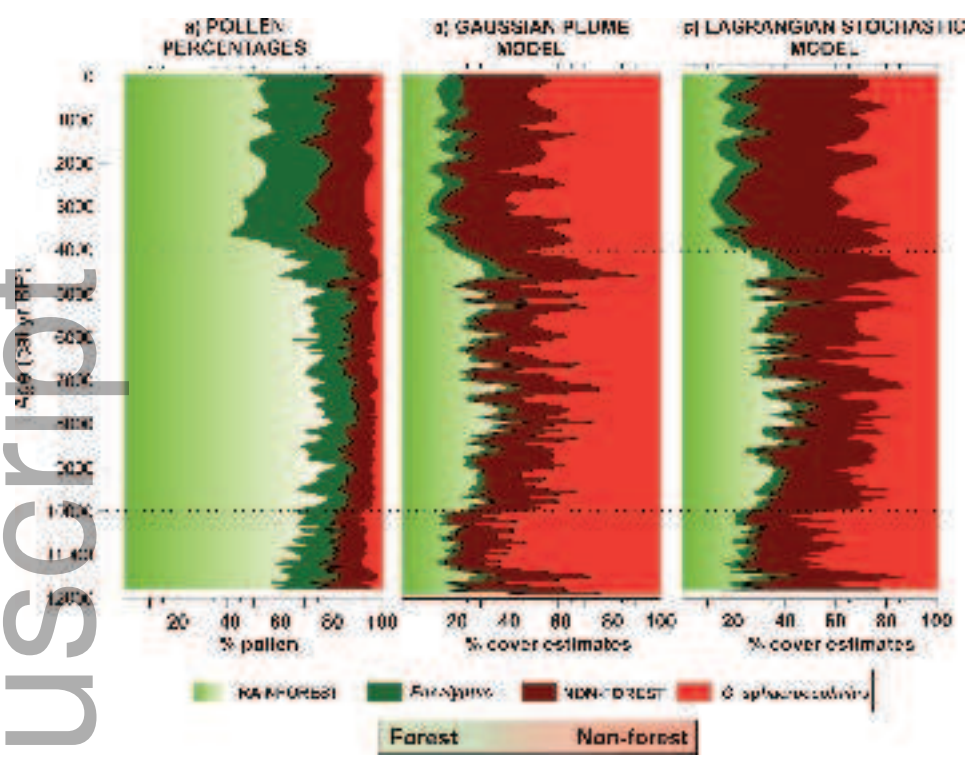
jbi_13040_f1.tif



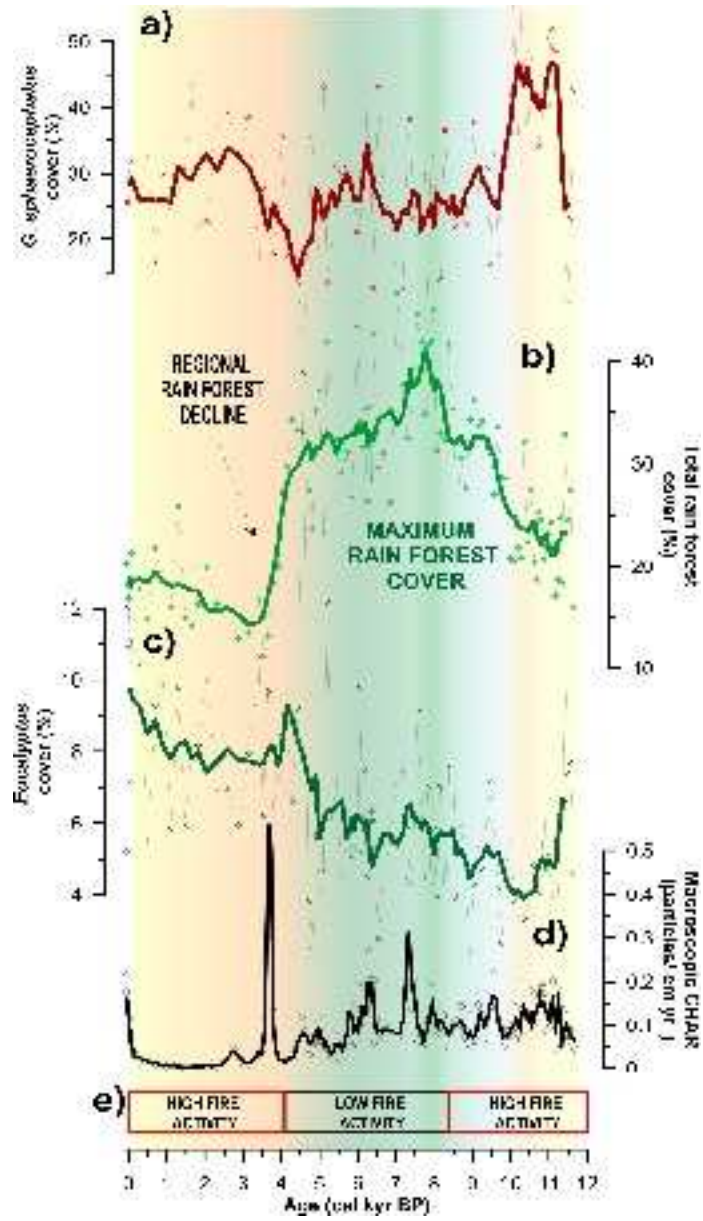
jbi_13040_f2.tif



jbi_13040_f3.tif



jbi_13040_f4.tif



jbi_13040_f5.tif